FILLING PROCESS IN AN OPEN TANK

S. L. Lee and S. R. Sheu
Department of Power Mechanical Engineering
National Tsing-Hua University
Hsinchu 30043
Taiwan

ABSTRACT

A numerical simulation for a filling process in an open tank is performed in this paper. A single set of governing equations is employed for the entire physical domain covering both water and air regions. The great density jump and the surface tension existing at the free surface are properly handled with the extended weighting function scheme and the NAPPLE algorithm. There is no need to smear the free surface. Through the use of a properly defined boundary condition, the method of "extrapolated velocity" is seen to provide accurate migrating velocity for the free surface, especially when the water front hits a corner or a vertical wall. Such a methodology does not pose to the Courant criterion, and thus allows large time steps. The numerical results show that when the water impinges upon a corner, a strong pressure gradient forms in the vicinity of the stagnation point. This forces the water to move upward along the vertical wall. The water eventually falls down and generates a gravity wave. These findings are seen to excellently agree with an existing experiment for the free surface evolution and the corresponding total water volume inside the tank. Due to its accuracy and simplicity, the present numerical method is believed to have good performances for simulating viscous free surface flow in industrial and environmental problems such as die-casting, cutting with water jet, gravity wave on sea surface, and many others.

INTRODUCTION

Filling process in cavity, mold, and tank is encountered in many scientific and industrial applications. The major difficulties dealing with such problems lie in the treatment of a few particular physical phenomena. First, an accurate tracking of the liquid-air interface (known as free surface) is needed. Second, turnaround of the liquid front should be properly handled when the liquid front impinges upon a corner or upon a wall perpendicular to the liquid flow. Third, the force balance equation on the free surface including the surface tension, the normal stress, and the shear stresses should be precisely satisfied. Fourth, dynamic contact angle at the liquid front should be carefully modeled unless the characteristic length of the problem is sufficiently large.

Many numerical simulation methods have been developed for mold-filling. However, the above-mentioned numerical difficulties are still not well resolved. Among them, Gilotte et al. (1995) determined the stream function inside the liquid

region with the potential flow theory, while a liquid jet was divided into branches manually. Instead of tracking the free surface, Advani and coworkers (Bruschke and Advani, 1994; Maier et al., 1996) located only the control volumes where the free surface was passing through. Local refinement thus was needed for a more precise free surface profile. Matsuhiro et al. (1990) and Zaidi et al. (1996) used the marker and cell method (MAC) to track the free surface advancement. Surface tension and stresses on the free surface were ignored. Sato and Richardson (1994) employed fringe elements in addition to fixed Cartesian fundamental elements such that the shape of the free surface could be tracked and then "boundary-fitted." Unfortunately, the speed of computation could be deteriorated when the fringe elements were too small due to a Courant-Friedrich-Lewy stability condition.

In their effort in resolving the free surface problem, Hirt and Nichols (1981) introduced the concept of VOF (volume of fluid). A scalar function $f(x,y,z,t)$ was defined such that f was zero in the air region and jumped to unity in the fluid region. Such a particular function was found governed by the hyperbolic equation (Hirt and Nichols, 1981)

$$\frac{\partial f}{\partial t} + u\frac{\partial f}{\partial x} + v\frac{\partial f}{\partial y} + w\frac{\partial f}{\partial z} = 0 \qquad (1)$$

where (u,v,w) denoted the flow velocity. Unfortunately, Eq. (1) is a trivial equation either in the liquid region or in the air region, while the VOF function f possesses a discontinuity at the free surface. This gives rise to a great numerical difficulty when Eq. (1) is solved. To circumvent the numerical difficulty, Hirt and Nichols (1981) employed the donor-acceptor scheme (Ramshaw and Trapp, 1976) to estimate the average f value inside each finite volume instead of solving Eq. (1) directly. However, the numerical procedure was found very tedious especially when applied to three-dimensional mold-filling problems (Chen et al., 1994). Furthermore, the time step should not be large due to the Courant criterion (advancement of the free surface should be less than one grid mesh in a single time step).

A few variants of the VOF function f have been proposed for solving Eq. (1) directly. They include at least the indicator function (Unverdi and Tryggvason, 1992), the marker function (Pericleous et al., 1995), the color function (Wu et al., 1996), the level set function (Sussman et al., 1998; Hetu and Ilinca, 1999), and the characteristic function (Pichelin and Coupez, 1999). All of these variant functions will be simply denoted

by f for convenience. Pichelin and Coupez (1999) employed an explicit discontinuous Taylor-Galerkin method (Pichelin and Coupez, 1998) to solve Eq. (1) for the characteristic function in a three-dimensional mold-filling problem. However, their methodology was found to produce an unphysical zigzag free surface.

In the use of the marker function, Pericleous and coworkers (Chan et al., 1991; Pericleous et al., 1995) employed the van Leer's TVD scheme to solve Eq. (1). Free surface with acute angles along with a serious numerical smearing was obtained. This does not seem physically realistic. The fundamental concept of the level set function is to use a smeared VOF function f instead of the original sharp step function such that the gradient of f exists across the free surface and thus Eq. (1) is numerically solvable. Very fine grids are generally needed. Otherwise, considerable artificial diffusion might arise. When applied to mold-filling problem, Dhatt et al. (1990) found that the choice of the spatial representation of f near the liquid front required experience, insight and personal adjustments. The identification of new fronts from the f-value required as well certain experience, especially for the corner region and highly curved fronts.

Very recehtly, Lee and Sheu (2000) proposed a new numerical formulation for free surface flow without smearing the free surface. A force balance equation considering the surface tension was imposed on the free surface through the use of the NAPPLE algorithm (Lee and Tzong, 1992). To achieve a smooth free surface profile, a particular technique called "extrapolated velocity" was developed. The results showed a good agreement with the well-documented dam-breaking experiments from Martin and Moyce (1952). In the present study, the methodology by Lee and Sheu (2000) is employed to simulate the filling process in an open tank. A modification to the method of "extrapolated velocity" will be performed to properly handle the sharp turnaround of the liquid front after its impingement on a corner of the tank.

THEORETICAL ANALYSIS

Consider a liquid being forced to fill a two-dimensional open tank of width L. The liquid enters the tank with a uniform velocity $U_{in}(t)$ through a gate of height B on one side of the tank as illustrated in Fig. 1. The flow is assumed laminar and incompressible. All of the physical properties of the liquid are constant. After introducing the dimensionless transformation

$$x = X/L, \quad y = Y/L, \quad u = U/U_c, \quad v = V/U_c,$$

$$p = (P - P_a)/(\rho_l U_c^2), \quad \tau = (U_c/L)t,$$

$$Re = \rho_l U_c L/\mu_l, \quad Fr = U_c/\sqrt{gL}, \quad \rho^* = \rho/\rho_l,$$

$$\mu^* = \mu/\mu_l, \quad b = B/L, \quad u_{in} = U_{in}/U_c \qquad (2)$$

a single set of governing equations covering both the liquid and the surrounding air can be written as

$$\frac{\partial u}{\partial x} + \frac{\partial v}{\partial y} = 0 \qquad (3)$$

$$\rho^* \left(\frac{\partial u}{\partial \tau} + u \frac{\partial u}{\partial x} + v \frac{\partial u}{\partial y} \right) = -\frac{\partial p}{\partial x}$$

$$+ \frac{1}{Re} \left(\frac{\partial}{\partial x} (\mu^* \frac{\partial u}{\partial x}) + \frac{\partial}{\partial y} (\mu^* \frac{\partial u}{\partial y}) \right) \qquad (4)$$

$$\rho^* \left(\frac{\partial v}{\partial \tau} + u \frac{\partial v}{\partial x} + v \frac{\partial v}{\partial y} \right) = -\frac{\partial p}{\partial y} - \frac{\rho^*}{Fr^2}$$

$$+ \frac{1}{Re} \left(\frac{\partial}{\partial x} (\mu^* \frac{\partial v}{\partial x}) + \frac{\partial}{\partial y} (\mu^* \frac{\partial v}{\partial y}) \right) \qquad (5)$$

The associated boundary conditions are

$$u(x,y,0) = 0, \quad v(x,y,0) = 0$$

$$u(0,y,\tau) = u_{in}(\tau) \text{ for } 0 \le y < b,$$

$$u(0,y,\tau) = 0 \text{ for } y \ge b,$$

$$v(0,y,\tau) = 0, \quad u(x,0,\tau) = 0, \quad v(x,0,\tau) = 0,$$

$$u(1,y,\tau) = 0, \quad v(1,y,\tau) = 0 \qquad (6)$$

Physically speaking, the boundary condition for the surrounding air does not have a significant influence on the liquid flow (Lee and Sheu, 2000). In addition, the filling process considered in the present study will terminate before the liquid reaches the height $y = 1$. Hence, the computational domain is truncated at $y = 1$ with the simplest artificial boundary condition

$$u(x,1,\tau) = 0, \quad \partial v(x,1,\tau)/\partial y = 0 \qquad (7)$$

Mathematically, the dimensionless density ρ^* and viscosity μ^* appearing in Eqs. (4) and (5) are step functions across the liquid-air interface. They have the value of unity in the liquid region and jump to another constant in the air region, i.e.

$$\rho^* = \begin{cases} 1 & \text{in liquid} \\ \rho_a/\rho_l & \text{in air} \end{cases} \qquad (8a)$$

$$\mu^* = \begin{cases} 1 & \text{in liquid} \\ \mu_a/\mu_l & \text{in air} \end{cases} \qquad (8b)$$

where the subscripts a and l denote, respectively, the properties of the air and the liquid. Note also that in the governing equations (3)-(5), the liquid-air interface is treated as an internal boundary such that no additional treatment is needed for the shear stresses there. In this connection, effect of surface tension is taken into account by considering the force balance equation on the liquid-air interface (Sarpkaya, 1996; Tsai and Yue, 1996; Lee and Sheu, 2000)

$$p_l = p_a + \frac{\kappa L}{We} + \frac{1}{Re} \left((\sigma_{nn})_l - (\frac{\mu_a}{\mu_l})(\sigma_{nn})_a \right) \qquad (9)$$

$$We = \frac{\rho_l U_c^2 L}{\gamma}, \quad \sigma_{nn} = 2 \frac{\partial v_n}{\partial n} \qquad (10)$$

where p_l and p_a stand for the dimensionless pressures on the liquid side and the air side, respectively. The symbols γ and κ are, respectively, the coefficient of surface tension and the curvature of a convex free surface profile. The notation σ_{nn} denotes the normal stress, while $\partial v_n/\partial n$ represents the normal strain rate. For convenience, the liquid-air interface will be referred to as "free surface" in the present study, although it is not really "free of stresses."

SOLUTION METHOD

In the present study, the momentum equations (4) and (5) are solved with the extended weighting function scheme (Lee and Sheu, 2000) on a fixed and nonstaggered Cartesian grid system. Due to the integration form of this particular scheme, the great discontinuity of the density ρ^* across the free surface can be effectively handled. It is noteworthy that both liquid and air could be incompressible even though their densities are significantly different. Thus, the law of "volume conservation" (3) is valid for the entire computational domain including the free surface itself and both regions of liquid and air. Through the use of the NAPPLE algorithm (Lee and Tzong, 1992; Lee and Sheu, 2000), the continuity equation (3)

is converted into a pressure-linked equation. The pressure solution then is solved with the SIS solver (Lee, 1989), while the force balance equation (9) is imposed on the free surface. The numerical procedure has been clearly described by Lee and Sheu (2000).

As mentioned earlier, one of the major difficulties in solving a moving free surface problem is the prediction of the free surface advancement. Generally speaking, when the solution (u, v, p) for a given time is obtained, the migrating velocity of the free surface cannot be precisely interpolated from the velocity solution at the grid points due to the great discontinuity of the velocity gradient across the free surface. In view of the fact that the velocity gradient on the liquid side is very small as compared to the air side, Lee and Sheu (2000) proposed the method of "extrapolated velocity from the liquid region" to estimate the migrating velocity of the free surface.

Figure 2 shows a schematic free surface (the solid curve) in a computational domain on a fixed Cartesian grid system. The grid points (the white nodes) adjacent to the free surface on the liquid side separate the computational domain into two regions. One of the two regions contains only liquid, while the other (the gray region) includes the whole air region, the free surface itself and a narrow liquid layer between the white nodes and the free surface. Based on the concept of the "extrapolated velocity" (Lee and Sheu, 2000), one solves the Laplace equations

$$\frac{\partial^2 u^*}{\partial x^2} + \frac{\partial^2 u^*}{\partial y^2} = 0, \qquad \frac{\partial^2 v^*}{\partial x^2} + \frac{\partial^2 v^*}{\partial y^2} = 0 \qquad (12)$$

on the gray region (see Fig. 2) with known velocities at the white nodes to yield an artificial velocity (u^*, v^*). The migrating velocity of the free surface is then interpolated from this artificial velocity.

As indicated by Lee and Sheu (2000), the Laplace equations (12) are used only to extrapolate the liquid velocity in a narrow region between the white nodes and the free surface. Influence of the boundary conditions imposed on the other boundaries of the computational domain (the gray region) would not be so significant. Hence, the following artificial boundary conditions are assigned for the boundaries when they are exposed to air

$$\partial v^*(0, y)/\partial x = 0, \quad \partial v^*(1, y)/\partial x = 0,$$
$$\partial u^*(x, 0)/\partial y = 0, \quad v^*(x, 0) = 0,$$
$$u^*(x, 1) = 0, \quad \partial v^*(x, 1)/\partial y = 0 \qquad (13)$$

Definition of the boundary conditions for u^* on the vertical walls $x = 0$ and $x = 1$ will be discussed later. After the artificial velocity (u^*, v^*) is known and the migration velocity of the free surface is obtained, the free surface advancement for the next time step can be easily estimated with a numerical procedure proposed by Lee and Sheu (2000).

RESULTS AND DISCUSSION

Hwang and Stoehr (1988) performed an experiment on filling process of water flow in a square cavity similar to the open tank shown in Fig. 1. The width of the tank and the height of the gate were $L = 15.2\,cm$ and $B = 3.8\,cm$, respectively. A sequence of photographs was taken to record the evolution of the free surface profile. However, the velocity at the gate $U_{in}(t)$ was not known. Fortunately, the volume of water inside the tank can be evaluated from the photographs. The result is approximately

$$Q(t) = 0.005\,t\,(6 - t) \qquad (14)$$

which implies

$$U_{in}(t) = 0.7896\,(1 - t/3) \qquad (15)$$

where Q, U_{in}, and t are measured in m^2, m/s and s, respectively.

In the present computation, the physical properties of water and air at $25°C$ are employed, i.e.

$$\rho_w = 998\,kg/m^3, \quad \mu_w = 0.99 \times 10^{-3}\,kg/m\,s$$
$$\rho_a = 1.205\,kg/m^3, \quad \mu_a = 1.81 \times 10^{-5}\,kg/m\,s$$
$$\rho_a/\rho_w = 0.001207, \quad \mu_a/\mu_w = 0.01828$$
$$\gamma = 0.0720\,N/m \qquad (16)$$

while the gravity is $g = 9.806\,m/s^2$. The characteristic velocity is assigned as

$$U_c = U_{in}(0) = 0.7896\,m/s \qquad (17)$$

The corresponding Reynolds number, Froude number, and Weber number are, respectively, $Re = 1.210 \times 10^5$, $Fr = 0.6468$, and $We = 1314$. The dimensionless gate height and inlet velocity are $b = 0.25$ and $u_{in}(\tau) = 1 - 0.06417\,\tau$, respectively.

Numerical results including the evolution of the free surface profile, velocity, and pressure were obtained on various combinations of grid meshes and time steps. Among them, the finest grid is $\Delta x = \Delta y = 0.0125$ and $\Delta \tau = 0.006493$ which corresponds to $0.19\,cm$ and $0.00125\,s$, respectively. It seems adequate for the present problem. The results obtained on the finest grid are revealed in Figs. 3 and 4.

Figure 3 shows the isobars (with increment $\Delta p = 0.1$) and the velocity at four representative times, i.e. $t = 0.1\,s$, $0.3\,s$, $0.45\,s$, and $0.65\,s$. Evolution of the free surface profile at every $0.05\,s$ is plotted in Fig. 4(a). To clearly observe the sharp advancement of the free surface in the period $0.2\,s \leq t \leq 0.3\,s$, the free surface is presented in Fig. 4(b) at every $0.01\,s$ in that period. The results reveal that the water enters the tank as a wall jet along the tank bottom on $y = 0$. After the water front hits the opposite wall on $x = 1$, a great pressure gradient forms in the vicinity of the stagnation point. This forces the water flow to jump up along the vertical wall on $x = 1$. It is quite interesting to note that after reaching the highest point ($y = 0.84$) at $t = 0.25\,s$, the water falls down and forms a gravity wave traveling in the $-x$ direction. It jumps up the vertical wall on $x = 0$ again after the wave reaches there. The computation was terminated at $t = 0.65\,s$ in view of the boundary condition (7). As expected, the air region is seen to possess essentially a uniform pressure.

It should be pointed out here that using a non-permeable condition

$$u^*(1, y) = 0 \qquad (18)$$

for the extrapolated velocity (u^*, v^*) will give rise to a physically unrealistic situation that the water front will never reach the opposite wall on $x = 1$. By contrast, the use of the freely permeable boundary condition

$$\partial u^*(1, y)/\partial x = 0 \qquad (19)$$

would cause a serious "water leakage" after the water hits the wall $x = 1$. Physically, the water does not "sense" the existence of the wall $x = 1$ before it reaches there. The boundary condition on the water front would suddenly transit from the "free surface" situation to a non-permeable condition. This instantly decelerates the water flow ($\partial u/\partial \tau \ll 0$) and thus induces a strong pressure increase in a region covering the stagnation point. In the present study, the freely permeable

boundary condition (19) is employed before the water reaches the wall $x = 1$, and thereafter, the non-permeable condition (18) is assumed. Suppose the water front just touches the wall at time τ^* during a time step elapsing in the period $\tau_{n-1} \leq \tau \leq \tau_n$. This particular time step will be divided into two sub-steps ($\tau^* - \tau_{n-1}$ and $\tau_n - \tau^*$) such that the freely permeable condition (19) can be applied exactly up to time τ^*. Similar treatment is performed when the gravity wave hits the wall $x = 0$.

To examine the reliability of the present numerical method, result of free surface advancement is compared with the experimental observation from Hwang and Storhr (1988) in Fig. 5. Excellent agreement between the present prediction and the experiment data is observable.

Finally, let the water volume inside the tank be examined in Fig. 6. The white dots in Fig. 6 are the water volume estimated from the experimental observation of Hwang and Steohr (1988). The dashed curve, a least-square approximation of the white dots, stands for the inlet condition (14) and (15) on which the present computation is based. The solid curve is the water volume directly evaluated from Fig. 4. From Fig. 6, one sees a satisfactory agreement between the solid curve and the dashed curve. This demonstrates the accuracy of the present numerical method on the law of mass conservation.

CONCLUSION

This paper presents a numerical simulation for a filling process in an open tank. A single set of governing equations is employed for the entire physical domain covering both water and air regions. The great density jump across the water-air interface (free surface) is handled with the extended weighting function scheme such that there is no need to smear the free surface. A force balance equation (including surface tension) is imposed on the free surface through the use of the NAPPLE algorithm. In this connection, a modified "extrapolated velocity" is developed to track the sharp turnaround of the water front when it impinges upon a corner. Excellent agreement between the present numerical results and an existing experiment is found. The numerical method employed in this work is very simple and accurate. It applies to industrial and environmental problems such as die-casting, cutting with water jet, gravity wave on sea surface, and many others as well.

ACKNOWLEDGMENTS

REFERENCES

Bruschke, M. V., and Advani, S. G., 1994, "A Numerical Approach to Model Non-Isothermal Viscous Flow Through Fibrous Media with Free Surfaces," *International Journal for Numerical Methods in Fluids*, Vol. 19, pp. 575-603.

Chan, K. S., Pericleous, K., and Cross, M., 1991, "Numerical Simulation of Flows Encountered during Mold-Filling," *Applied Mathematical Modelling*, Vol. 15, pp. 624-631.

Chen, C. W., Li, C. R., Han, T. H., Shei, C. T., Hwang, W. S., and Houng, C. M., 1994, "Numerical Simulation of Filling Pattern for an Industrial Die Casting and Its Comparison with the Defects Distribution of an Actual Casting," *Transactions of the American Foundrymen's Society*, Vol. 104, pp. 139-146.

Dhatt, G., Gao, D. M., and Cheikh, A. B., 1990, "A Finite Element Simulation of Metal Flow in Moulds," *International Journal for Numerical Methods in Engineering*, Vol. 30, pp. 821-831.

Gilotte, P., Huynh, L. V., Etay, J., and Hamar, R., 1995, "Shape of the Free Surfaces of the Jet in Mold Casting Numerical Modeling and Experiments," *ASME Journal of Engineering Materials and Technology*, Vol. 17, pp. 82-85.

Hetu, J.-F., and Ilinca, F., 1999, "A Finite Element Method for Casting Simulations," *Numerical Heat Transfer*, Vol. 36A, pp. 657-679.

Hirt, C. W., and Nichols, B. D., 1981, "Volume of Fluid (VOF) Method for the Dynamics of Free Boundaries," *Journal of Computational Physics*, Vol. 39, pp. 201-225.

Hwang, W.-S., and Stoehr, R. A., 1988, "Modeling of Fluid Flow," in *Metal Handbook (9th edition)*, Vol. 15, pp. 867-876.

Lee, S. L., 1989, "A Strongly-Implicit Solver for Two-Dimensional Elliptic Differential Equations," *Numerical Heat Transfer*, Vol. 16B, pp. 161-178.

Lee, S. L., and Sheu, S. R., 2000, "A New Numerical Formulation for Incompressible Viscous Free Surface Flow without Smearing the Free Surface," *International Journal of Heat and Mass Transfer*, (in press).

Lee, S. L., and Tzong, R. Y., 1992, "Artificial Pressure for Pressure-Linked Equation, *International Journal of Heat and Mass Transfer*, Vol. 35, pp. 2705-2716.

Maier, R. S., Rohaly, T. F., Advani, S. G., and Fickie, K. D., 1996, "A Fast Numerical Method for Isothermal Resin Transfer Mold Filling," *International Journal for Numerical Methods in Engineering*, Vol. 39, pp. 1405-1417.

Martin, J. C., and Moyce, W. J., 1952, "An Experimental Study of the Collapse of Liquid Columns on a Rigid Horizontal Plane," *Philos. Trans. Roy. Soc. London*, Vol. 244A, pp. 312-324.

Matsuhiro, I, Shiojima, T, Shimazaki, Y, and Daiguji, H., 1990, "Numerical Analysis of Polymer Injection Moulding Process Using Finite Element Method with Marker Particles," *International Journal for Numerical Methods in Engineering*, Vol. 30, pp. 1569-1576.

Pericleous, K. A., Chan, K. S., and Cross, M., 1995, "Free Surface Flow and Heat Transfer in Cavities: the SEA Algorithm," *Numerical Heat Transfer*, Vol. 27B, pp. 487-507.

Pichelin, E., and Coupez, T., 1998, "Finite Element Solution of the 3D Mold Filling Problem for Viscous Incompressible Fluid," *Computer Methods in Applied Mechanics and Engineering*, Vol. 163, pp. 359-371.

Pichelin, E., and Coupez, T., 1999, "A Taylor Discontinuous Galerkin Method for the Thermal Solution in 3D Mold Filling," *Computer Methods in Applied Mechanics and Engineering*, Vol. 178, pp. 153-169.

Sarpkaya, T., 1996. "Vorticity, Free Surface, and Surfactants," *Annular Review of Fluid Mechanics*, Vol. 28, pp. 83-128.

Sato, T., and Richardson, S. M., 1994, "Numerical Simulation Method for Viscoelastic Flows with Free Surfaces—Fringe Element Generation Method," *International Journal for Numerical Methods in Fluids*, Vol. 19, pp. 555-574.

Sussman, M., Fatemi, E., Smereka, P, and Osher, S., 1998, "An Improved Level Set Method for Incompressible Two-Phase Flows," *Computers and Fluids*, Vol. 27, pp. 663-680.

Tsai, W. T., and Yue, D. K. P., 1996, "Computation of Nonlinear Free-Surface Flows," *Annular Review of Fluid Mechanics*, Vol. 28, pp. 249-278.

Unverdi, S. O., and Tryggvason, G., 1992, "A Front-Tracking Method for Viscous, Incompressible, Multi-Fluid Flows," *Journal of Computational Physics*, Vol. 100, pp. 25-37.

Wu, J., Yu, S. T., and Jiang, B. N., 1996, "Simulation of Two-Fluid Flows by the Least-Square Finite Element Methods Using a Continuum Surface Tension Model," NASA CR-202314 (Lewis Research Center, Cleveland, Ohio).

Zaidi, K, Abbes, B., and Teodosiu, C., 1996, "Finite Element Simulation of Mold Filling Using Marker Particles and $k-\varepsilon$ Model of Turbulence," *Computer Methods in Applied Mechanics and Engineering*, Vol. 134, pp. 241-247.
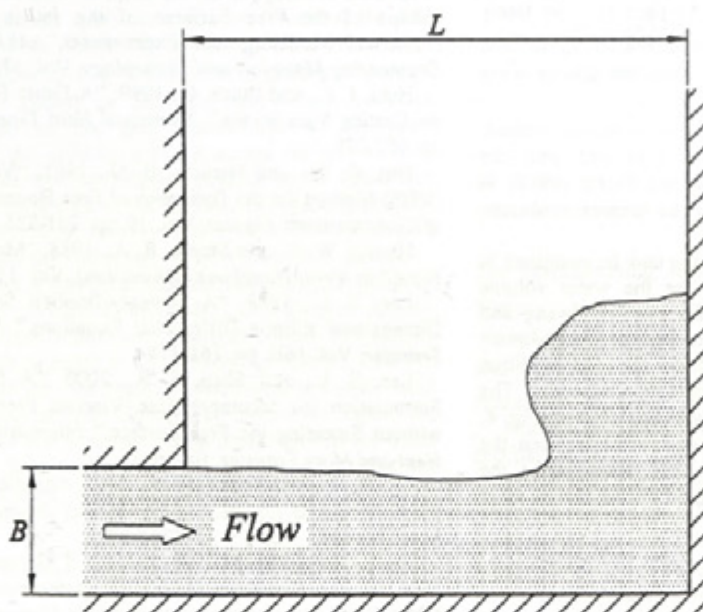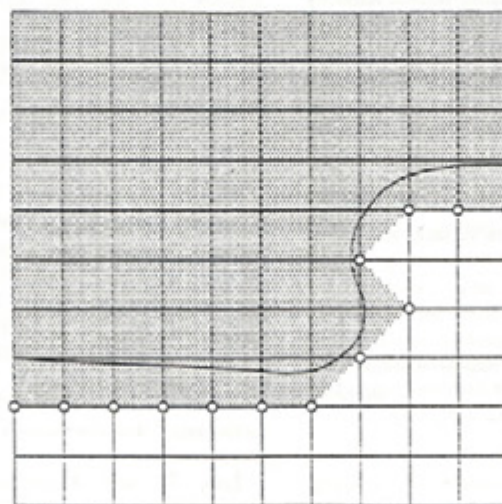
Fig. 1 Configuration of the problem

Fig. 2 Computational domain for the artificial velocity (u^*, v^*)
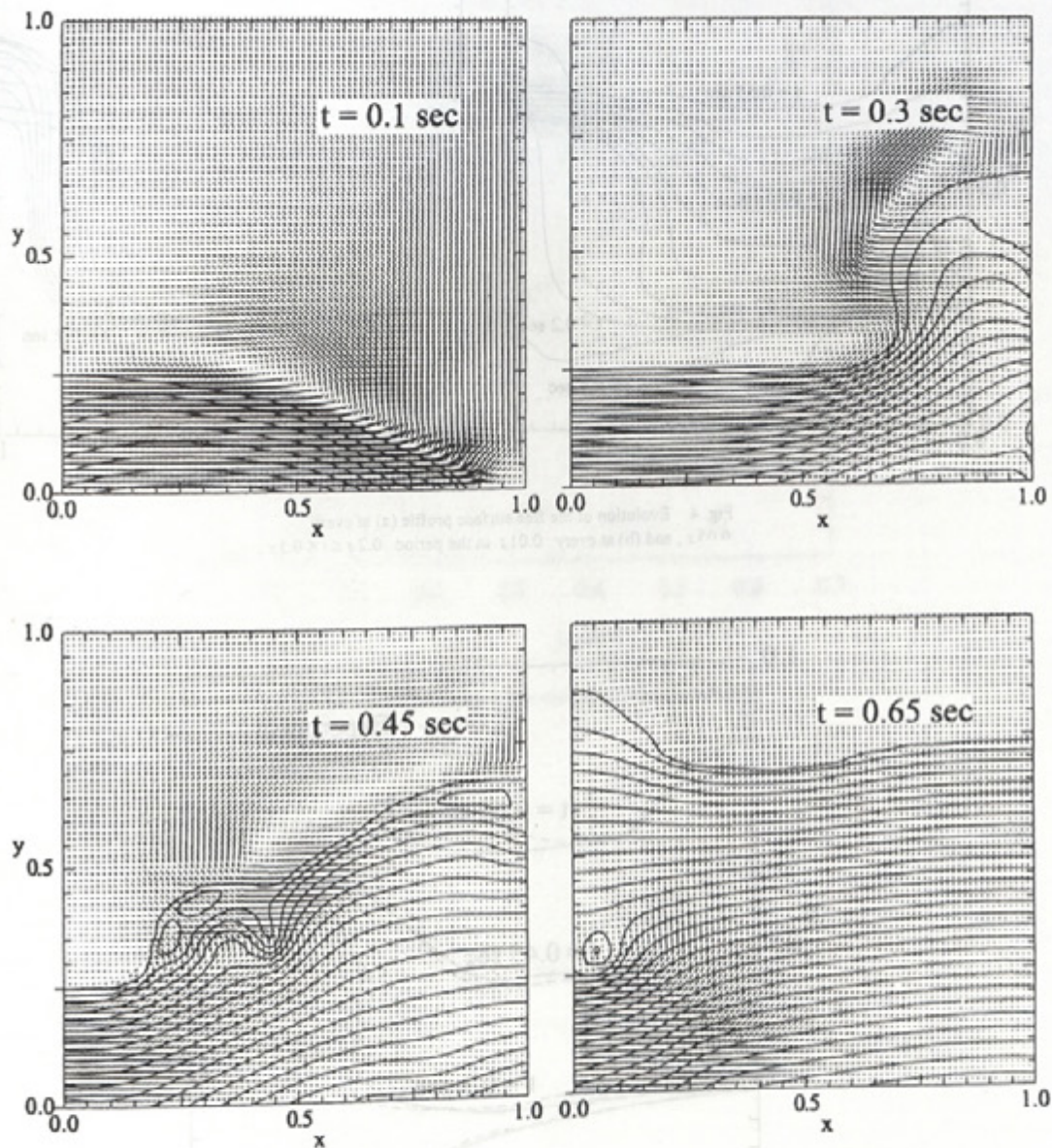
Fig. 3   The isobars (with increment $\Delta p = 0.1$) and the
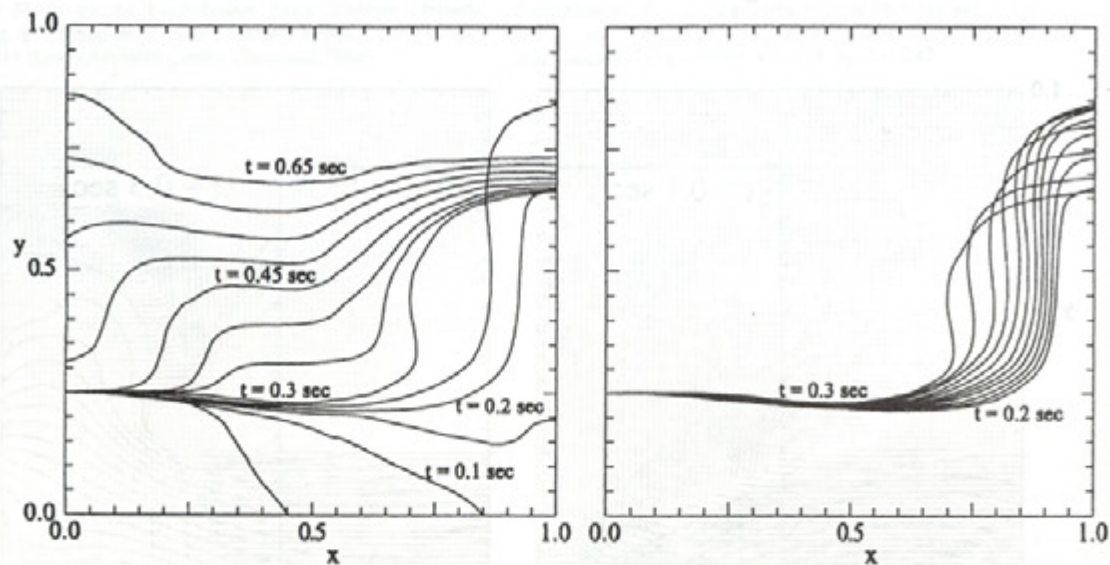velocity vectors at four representative times.

Fig. 4   Evolution of the free surface profile (a) at every
0.05 s , and (b) at every 0.01 s in the period $0.2 s \leq t \leq 0.3 s$.
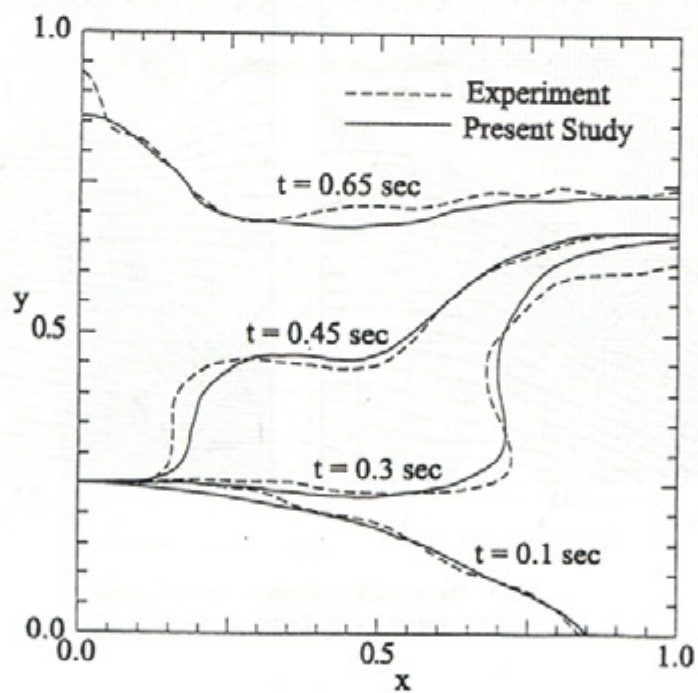

Fig. 5   Comparison of free surface advancement between the
present result and the experimental observation (Hwang and
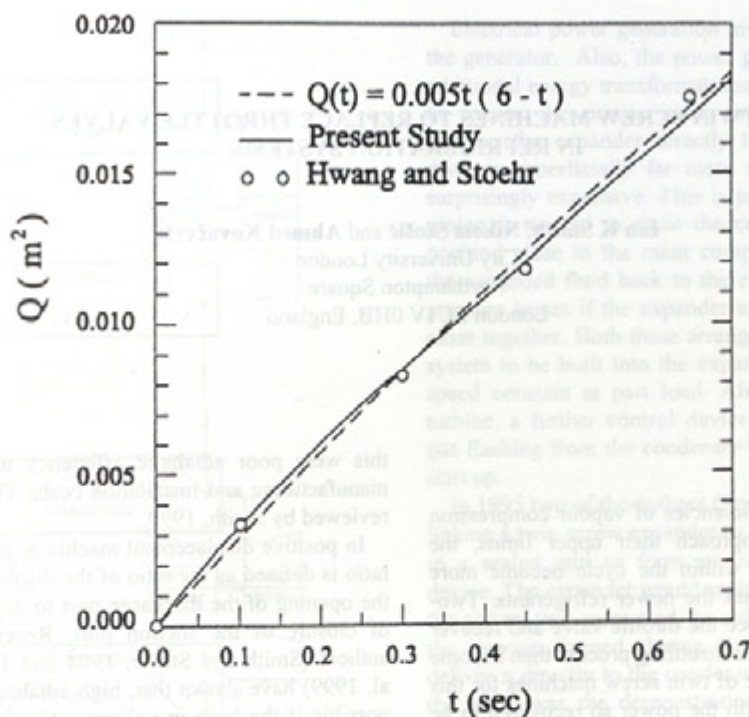Storhr, 1988)

Fig. 6 An examination of the computed mass conservation
inside the tank